

First-principles study on the magnetic properties of ordered $\text{Nd}_6(\text{Fe,Ga})_{14}$ alloys

Kazushige Hyodo,¹ Yuta Toga,² and Akimasa Sakuma¹

¹*Department of Applied Physics, Tohoku University, Aoba 6-6-05, Aoba-ku, Sendai, Japan*

²*ESICMM, National Institute for Materials Science, Sengen 1-2-1, Tsukuba, Japan*

We studied the stable magnetic structure of ordered $\text{Nd}_6\text{Fe}_{14-x}\text{Ga}_x$ ($x = 0, 1$) alloys, which appears in the grain-boundary (GB) phase of Nd-Fe-B permanent magnets, using first-principles techniques. Slight Ga doping ($x = 1$) was shown to contribute to the stabilization of an anti-ferromagnetic (AF) state, whereas the non-doped case ($x = 0$) was revealed to favor ferromagnetic state rather than AF state with a slight energy difference.

The intermetallic compounds $R_6\text{Fe}_{14-x}M_x$ (R =rare earth, M =Si, Ga, Al, Ge, Cu etc.) have attracted attention due to their interesting properties such as metamagnetic transition at a few Tesla of magnetic field^{1,2} and large magnetic anisotropy field larger than 7 T.³ Also, in technological viewpoints, these alloys were intensively investigated because their existence as grain boundary (GB) phase in Nd-Fe-B permanent magnets enhances the coercive force H_c ,^{4,5} and they absorb large amount of hydrogens without any change of symmetry.^{6,7} Quite recently, the effects of $\text{Nd}_6\text{Fe}_{14-x}\text{Ga}_x$ as a GB phase in Nd-Fe-B magnets has been revisited,⁸ since the higher H_c of Nd-Fe-B magnets is in great demand for realizing more energy-efficient motors. In particular, motors in recent electric vehicles that operate under high temperature require a larger H_c to suppress thermal fluctuations of the magnetization.

Besides these attractive properties, the magnetic structure has not yet been established and has so far been controversy. Experimentally, various measurements were performed, such as Mössbauer measurement,^{1,5,6,9,10,15} neutron^{11,12} and X-ray diffractions.^{9,10,13-15} The neutron and some measurements^{5,12-14} proposed that the $R_6\text{Fe}_{14-x}M_x$ form antiferromagnetic (AF) structure, while other experiments suggested ferri-⁹⁻¹¹ or ferromagnetic structures.³ In addition, the reported magnetic moments on Fe sites were different depending on the experimental methods.^{16,17} In order to gain insight into the magnetism of this alloy, the first principles calculations for the electronic and magnetic structures could be helpful.

In the present study, we focus on the $\text{Nd}_6\text{Fe}_{13}\text{Ga}$ alloy and investigated the magnetic properties of this system using the first-principles technique. The main purpose of this work is to determine the magnetic structure including magnetic moments on each Fe site and the next is to examine its stability, in order to provide helpful information to understand the role of these alloys as a GB phase in Nd-Fe-B magnets. For the latter aim, we are concerned with the effects of Ga atoms on the magnetism of this system. To see this, we examined also the magnetic structure of hypothetical $\text{Nd}_6\text{Fe}_{14}$ alloy which may be unstable to exist alone, and compared it with that of $\text{Nd}_6\text{Fe}_{13}\text{Ga}$.

Since the crystal structure of $\text{Nd}_6\text{Fe}_{13}\text{Ga}$ is quite complex and the number of atoms in the unit cell is so large, there exist infinite possibilities in magnetic structure. Therefore, we concentrate ourselves to the AF structure proposed by neutron measurement¹² as a candidate of the magnetic structure, and investigate the stability of the AF structure. It was found, as a result of the present studies, that $\text{Nd}_6\text{Fe}_{14}$ alloy favors ferromagnetic state rather than AF state with a slight energy difference, and the substitution of Fe atoms by Ga atoms makes the AF state much stable, leading to $\text{Nd}_6\text{Fe}_{13}\text{Ga}$. We also revealed that this stable AF state originated from the anti-parallel magnetic coupling between the neighboring Nd-Fe blocks shown in Fig. 1 and few magnetism of the doped Ga contributed to the stabilization of this magnetic state.

The unit cell of the ordered $\text{Nd}_6\text{Fe}_{14-x}\text{Ga}_x$ ($x = 0, 1$) system consists of 80 atoms, as shown in Fig. 1, according to a previous experimental report.¹⁸ When $x = 1$, the doped Ga atoms replace the $4a$ Fe atoms (see Fig. 1). We adopted the displayed FM and AF states shown in Fig. 1 as candidates for stable magnetic states. The characteristic magnetic structure of the AF state is based on the observed AF state in $\text{Nd}_6\text{Fe}_{12}\text{Ga}_2$ alloys.¹² In both states, the magnetic moments of the internal atoms in the Nd-Fe blocks and Fe(Ga) layers are parallel, as shown by the arrow in Fig. 1. In contrast, the magnetic moments of the adjacent Nd-Fe block are parallel in the FM state and anti-parallel in the AF state.

We used the Vienna ab initio simulation package (VASP 5.4.1) as a first-principles calculation method for obtaining the total energy.²⁰ The cell volume, lattice constants, and internal atom positions were redefined from the experimental values¹⁸ using the self-consistent relaxation operation in each composition and magnetic state. The cut-off energy is 334.9 eV, and the Monkhorst-Pack \mathbf{k} -point meshes are $5 \times 5 \times 3$ in collinear calculations and $3 \times 3 \times 1$ in non-collinear calculations. A self-consistent electronic structure was obtained for valence electrons, except for the $4f$ electrons in the Nd atoms, which were treated as core electrons in this study. The ionic potentials is described by the plane-augmented-wave (PAW) method,^{21,22} and the exchange-correlation energy of the valence electrons is represented within the generalized

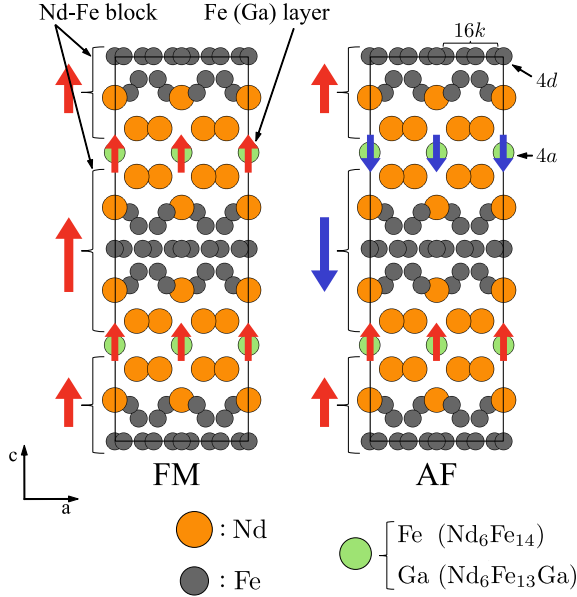


FIG. 1. Unit cell and candidates of stable magnetic structures of ordered $\text{Nd}_6\text{Fe}_{14}$ and $\text{Nd}_6\text{Fe}_{13}\text{Ga}$. The green circles indicate the atomic positions denoted by $4a$, which are occupied by Ga or Fe atoms in $\text{Nd}_6\text{Fe}_{13}\text{Ga}$ or $\text{Nd}_6\text{Fe}_{14}$, respectively. The top, bottom and central layers are constituted of $4d$ and $16k$ Fe atoms. These crystal structures were drawn using VESTA.¹⁹

gradient approximation (GGA), whose specific form was given by Ceperly and Alder and parametrized by Perdew et al.²³

Table I (a) shows the lattice constant of each magnetic state after the relaxation process in both alloys. The obtained lattice constants are almost equal between the two alloys and the two magnetic states. In addition, the obtained relaxed value of the AF state in $\text{Nd}_6\text{Fe}_{13}\text{Ga}$ is almost the same as the experimental value ($a = 8.069 \text{ \AA}$ and $c = 22.937 \text{ \AA}$,¹⁸ the differences are about 0.8%).

In table I (b), using the relaxed atomic positions, we show the calculated energy of the FM and AF states (E_{FM} , E_{AF}) and the difference of them, $\Delta E = E_{\text{FM}} - E_{\text{AF}}$. Additionally in this study, for convenience in comparison among different systems, we defined the interface magnetic coupling energy:

$$J = \frac{E_{\text{FM}} - E_{\text{AF}}}{2S}, \quad (1)$$

where S is the interface area of the Nd-Fe block in the case of AF state (the difference of the square area between the FM and AF states is less than 1% in both alloys, as shown in table I (a)). Note that two interfaces between Nd-Fe blocks exist in the unit cell. Positive (negative) J indicates preference of the AF (FM) state over the FM (AF) state. These results in table I (b) indicated that the $\text{Nd}_6\text{Fe}_{13}\text{Ga}$ prefer AF states whereas the $\text{Nd}_6\text{Fe}_{14}$ favours FM state with a slight energy difference.

To further understand the energetic preference between the AF and FM states in the $\text{Nd}_6\text{Fe}_{14-x}\text{Ga}_x$ ($x =$

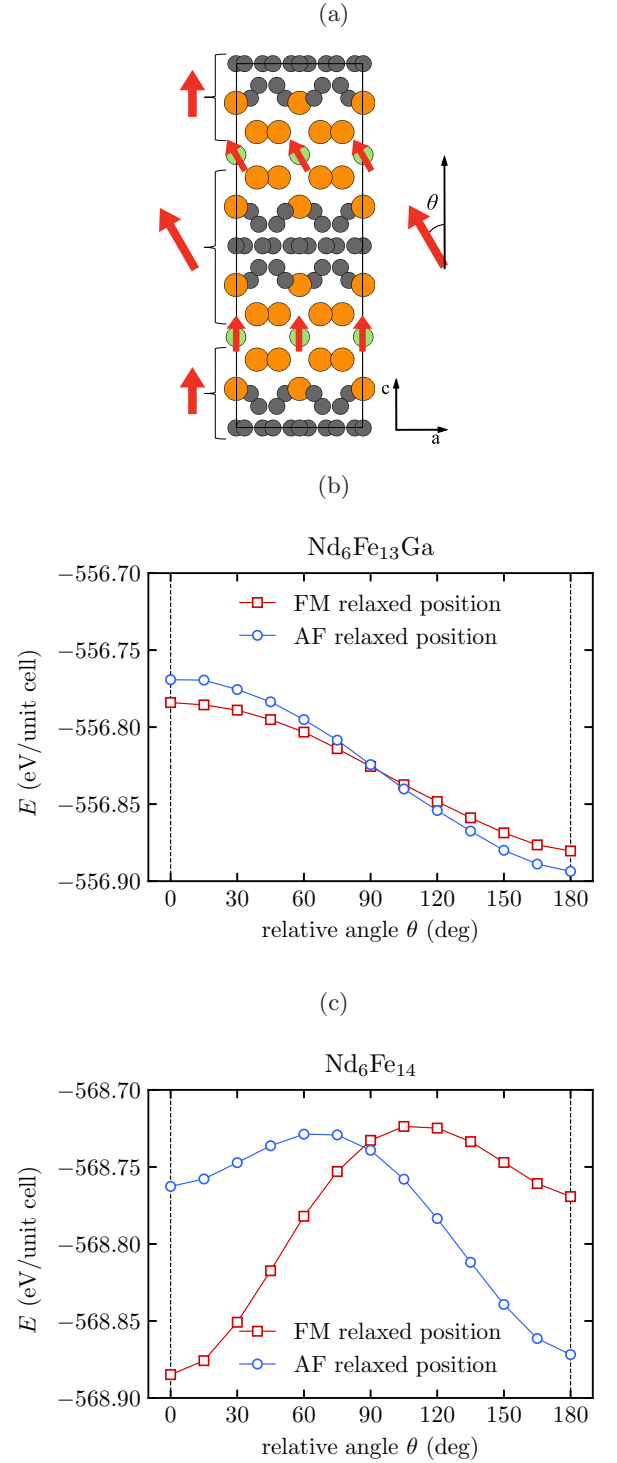


FIG. 2. (a) Our considered magnetic configuration, where the magnetic moments in half of the Nd-Fe blocks and Fe(Ga) layers have a relative angle θ to the magnetic moments of the other blocks and other layers. (b) Calculated energy of the unit cell in $\text{Nd}_6\text{Fe}_{13}\text{Ga}$ in each condition of θ . (c): Calculated energy of the unit cell in $\text{Nd}_6\text{Fe}_{14}$ in each condition of θ .

TABLE I. (a): Obtained lattice constants along the a - and c -axes after the relaxation process in the AF and FM states of $\text{Nd}_6\text{Fe}_{13}\text{Ga}$ and $\text{Nd}_6\text{Fe}_{14}$. The lattice constant along the b -axis is same as that along the a -axis due to the symmetry of this system. (b): Calculated energies in the FM (E_{FM}) and the AF (E_{AF}) states for the unit cell shown in Fig. 1 and the difference between them, ΔE . Interface coupling energy, J , defined by Eq. (1).

(a)	
	a (\AA) c (\AA)
$\text{Nd}_6\text{Fe}_{13}\text{Ga}(\text{FM})$	8.004 23.209
$\text{Nd}_6\text{Fe}_{13}\text{Ga}(\text{AF})$	8.006 23.119
$\text{Nd}_6\text{Fe}_{14}(\text{FM})$	7.986 22.959
$\text{Nd}_6\text{Fe}_{14}(\text{AF})$	8.004 22.773

(b)				
	E_{FM} (eV)	E_{AF} (eV)	ΔE (eV)	J (mJ/m ²)
$\text{Nd}_6\text{Fe}_{13}\text{Ga}$	-556.752	-556.891	0.139	8.7
$\text{Nd}_6\text{Fe}_{14}$	-568.867	-568.846	-0.021	-1.3

0, 1) system, we calculated the energy of assumed non-collinear magnetic moments, which continuously changed from the FM to AF state. Figure 2 (a) shows our considered magnetic structure, where the magnetic moments in half of the Fe-Nd blocks and Fe(Ga)-layers are rotated by an angle θ from those in the other blocks and layers. Figure 2 (b) and (c) present the obtained energy of $\text{Nd}_6\text{Fe}_{13}\text{Ga}$ and $\text{Nd}_6\text{Fe}_{14}$ as a function of θ . The red and blue lines shows the calculation results under the relaxed atomic positions in the FM and AF states, respectively. The case of $\theta = 0^\circ$ ($\theta = 180^\circ$) in each figure corresponds to the FM (AF) state in Fig. 1. Note that the energies in these cases are a slight decrease from the results in Table I (b), which is owing to the non-collinear spin configurations. Even if total moment is along c -axis, the spins are not completely collinear but slightly inclined to each other, and reduce the energies. Although the non-collinear calculation condition may reduce the results of $|J|$ by about 30% at maximum, the change does not affect the discussion in this study.

In $\text{Nd}_6\text{Fe}_{13}\text{Ga}$ (Fig. 2 (b)), the $\theta = 180^\circ$ and $\theta = 0^\circ$ cases correspond to the minimum and maximum points, respectively, and the obtained energy monotonically decreases with the increase of θ . In addition, this trend is shown in both lines, which indicate that the magnetic structure shifts to the AF state, regardless of the atomic positions. Thus, we confirmed that the AF state was preferred over the FM state in $\text{Nd}_6\text{Fe}_{13}\text{Ga}$. In contrast, in $\text{Nd}_6\text{Fe}_{14}$ (Fig. 2 (c)), the dependence of energy on θ was found to differ between cases with different atomic positions; if a stable atomic position is adopted in the FM state, the FM state ($\theta = 0^\circ$) becomes the ground state, whereas the AF state ($\theta = 180^\circ$) becomes the ground state for atomic positions in the AF state. This result indicates that the stable magnetic structure easily

TABLE II. Calculated energy of the FM and AF states (E_{FM} and E_{AF}) for the unit cell, the difference between them $\Delta E = E_{\text{FM}} - E_{\text{AF}}$, and the interface coupling energy J in $\text{Nd}_6\text{Fe}_{13}M$ ($M = \text{Si}, \text{Al}, \text{empty}$).

M	E_{FM} (eV)	E_{AF} (eV)	ΔE (eV)	J (mJ/m ²)
Al	-557.908	-558.056	0.148	9.2
Si	-567.891	-568.149	0.258	16.2
empty	-536.742	-536.875	0.133	8.3

changes depending on the atomic position in $\text{Nd}_6\text{Fe}_{14}$, even though the FM state is rather stable compared to the AF state in this structure, as shown in table I (b).

Next, we investigated the role of Ga atoms on the AF structure in $\text{Nd}_6\text{Fe}_{13}\text{Ga}$. We focused on the almost non-magnetism of the doped Ga atom of $\text{Nd}_6\text{Fe}_{13}\text{Ga}$, whose magnetic moments were $0.0\mu_{\text{B}}$ /atom (see later in Table III) in both the AF and FM states, respectively. From this result, it would be reasonable to presume that the stable AF state in $\text{Nd}_6\text{Fe}_{13}\text{Ga}$ (Fig. 1) is almost dominated by the AF coupling between the neighboring Nd-Fe blocks and hardly relates to the magnetic interaction mediated by Ga atoms. To demonstrate this hypothesis, we compared the stability of the AF state in $\text{Nd}_6\text{Fe}_{13}M$, where the Ga atoms in $\text{Nd}_6\text{Fe}_{13}\text{Ga}$ were replaced by some non-magnetic M atoms or empty space. Table II shows the calculated energies of the FM and AF states and the evaluated interface coupling J using Eq. (1) in $\text{Nd}_6\text{Fe}_{13}M$ ($M = \text{Al}, \text{Si}, \text{empty}$). The results of $M = \text{Al}, \text{Si}$ were calculated from the relaxed atomic positions, which was obtained with respect to each system and magnetic state. In the case of $M = \text{empty}$, we used the relaxed atomic position of $\text{Nd}_6\text{Fe}_{13}\text{Ga}$ and removed the Ga atoms with holding the other atomic positions fixed.

We found that all obtained J values were positive values. The preference of the AF state in the case of $M = \text{Si}$, as well as the case of $\text{Nd}_6\text{Fe}_{13}\text{Ga}$, coincides with the observed result in previous experiments.^{13,14} In addition, the obtained J values are similar between these systems. Especially, the case of $M = \text{empty}$ has almost same value as $\text{Nd}_6\text{Fe}_{13}\text{Ga}$ under the same structure without Ga. From these results, we conclude that the role of Ga is only as a spacer and the stability of the AF state in $\text{Nd}_6\text{Fe}_{13}\text{Ga}$ mainly originates from the anti-parallel coupling between the neighboring Nd-Fe blocks. At this stage, we consider that this anti-parallel coupling is mainly attributed to a kind of kinetic exchange interaction (such as RKKY interaction in most RE metals) between the Nd layers on both sides of the Ga $4a$ layer, which is mediated by s - or p - electrons.

For more detailed studies of the substitution effect of the Ga $4a$ atoms, the calculated magnetic moments, m_s , on each site for $M = \text{Ga}, \text{Al}, \text{Si}, \text{and Fe}$ are listed in Table III, together with the experimental data, for comparison. And, we also added the calculation result of a $\text{Pr}_6\text{Fe}_{13}\text{Si}$ system to compared with the experiment for

TABLE III. Theoretical (this work, used Bader charge analysis^{24,25}) and previous experimental (Mössbauer measurement (MS) or neutron diffractions (ND)) results of the amplitude of magnetic moment, m_s , for each Fe ion in some $R_6\text{Fe}_{13}M$ systems. All theoretical results were evaluated in the stable (only $\text{Nd}_6\text{Fe}_{14}$ is the FM, and the others are the AF) states and in the relaxed atomic positions.

$R_6\text{Fe}_{13}M$	m_s (μ_B)				
	Fe				M
	$4d$	$16k$	$16l_1$	$16l_2$	$4a$
Theory					
$\text{Nd}_6\text{Fe}_{13}\text{Ga}$	1.95	2.24	2.15	2.28	0.00(3)
$\text{Nd}_6\text{Fe}_{13}\text{Al}$	1.96	2.25	2.16	2.30	0.00(4)
$\text{Nd}_6\text{Fe}_{13}\text{Si}$	1.97	2.23	2.15	2.30	0.00(3)
$\text{Pr}_6\text{Fe}_{13}\text{Si}$	2.05	2.27	2.17	2.35	0.00(2)
$\text{Nd}_6\text{Fe}_{14}$	1.94	2.23	2.15	2.25	2.31
Experiment					
$\text{Nd}_6\text{Fe}_{13}\text{Si}@2\text{K}$ (ND) ¹⁶	2.8	2.6	2.4	1.8	-
$\text{Nd}_6\text{Fe}_{13}\text{Si}@4.2\text{K}$ (MS) ¹⁶	2.5	2.3	2.1	1.6	-
$\text{Pr}_6\text{Fe}_{13}\text{Si}@1.5\text{K}$ (ND) ¹⁷	0.9	2.0	2.1	2.1	-
$\text{Nd}_6\text{Fe}_{13}\text{Au}@1.5\text{K}$ (ND) ¹⁷	1.3	2.6	2.6	2.6	-

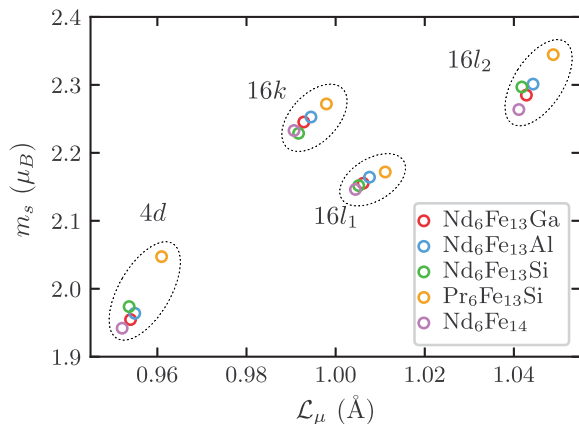


FIG. 3. The relationship between the canonical bond length, \mathcal{L}_μ , defined by Eq. (2) and the magnetic moment, m_s , for each of the atoms and the substances.

the same substance. One may notice that the Fe magnetic moments at each site have almost same values irrespective of substance except for the $\text{Pr}_6\text{Fe}_{13}\text{Si}$. The slightly differences of the $\text{Pr}_6\text{Fe}_{13}\text{Si}$ is due to changes in the space of each Fe site (see later and Fig. 3). On the other hand, the remarkable difference can be found in the moment on $4d$ Fe site between the calculated and experimental values; the moment on the $4d$ site is the smallest in the calculated and the two experimental data at the bottom of Table III, while one is the largest value in the other two experimental data. We have confirmed that the trend in which the moment on $4d$ site is the smallest can be seen also in other calculation method (Korringa-Kohn-Rostoker method) for electronic structure.²⁶

Within the framework of electronic structure calculations, we take the trend owing to the situation that the $4d$ Fe moments are surrounded relatively densely by other Fe sites such as $16k$, $16l_1$ and $16l_2$ sites, resulting in strong itinerant character and the small magnetic moments. To analyze this, we adopted a canonical bond length proposed by Harashima et al.²⁷ as follow:

$$\mathcal{L}_\mu = \frac{1}{2} \left(\sum_\nu |\mathbf{r}_\mu - \mathbf{r}_\nu|^{-10} \right)^{-\frac{1}{10}}, \quad (2)$$

here μ and ν are atom indices, and \mathbf{r} is an atom position vector. This length is based on the canonical band theory²⁸ and formulated from d - d hopping integral. Since magnetic moment is mainly contributed by the d -electrons, thus \mathcal{L}_μ is reasonable to compare the atomic spaces with the magnetic moments.

Figure 3 shows clearly positive correlation between \mathcal{L}_μ and m_s for each of the atoms and the substances. For $\text{Pr}_6\text{Fe}_{13}\text{Si}$, it can be understood that the increase of \mathcal{L}_μ reflect the slightly difference of m_s in Table III. The canonical length is not possible to explain the reverse magnitude relationship between $16k$ and $16l_1$, whereas \mathcal{L}_{4d} is definitely smaller than the others, which support that the moment on $4d$ site is the smallest in Table III.

Finally, we examined the origin of competition between the FM and AF states in the $\text{Nd}_6\text{Fe}_{14}$ system. From Table III and Fig. 3, it is confirmed that the $\text{Nd}_6\text{Fe}_{14}$ is almost same as the $\text{Nd}_6\text{Fe}_{13}\text{Ga}$ regarding m_s and \mathcal{L}_μ except for m_s of $4a$ site. The difference of magnetism between them mainly depends on the $4a$ site irrespective of the structures. In this discussion, therefore, in addition to the AF coupling between the Nd-Fe blocks, we paid attention to the magnetic interactions that arose from the $4a$ Fe layers in Fig. 1 because the magnetic moments of these Fe atoms reached $2.3\mu_B/\text{atom}$ (see Table III) in both the FM and AF states. To estimate the magnetic coupling related to these $4a$ Fe layers, we assumed the non-collinear magnetic structure exhibited in Fig. 4 (a), where the magnetic moments of the $4a$ Fe layers were rotated by an angle θ from those of Nd-Fe blocks. Figure 4 (b) shows the calculated energy of $\text{Nd}_6\text{Fe}_{14}$ as a function of θ . The atomic position was fixed at the relaxed value of the FM state in Fig. 1, which corresponded to the $\theta = 0$ condition in Fig. 4 (a). We found that the calculated energy became unstable with increasing θ ; this result indicates that parallel magnetic couplings exist between the Nd-Fe blocks and the $4a$ Fe layers. From the energy difference between $\theta = 0^\circ$ and $\theta = 180^\circ \sim 0.4$ eV/unitcell in Fig. 4 (b), the parallel magnetic coupling can be evaluated as $J_{\text{NdFe}/\text{Fe}} \sim -12.5$ mJ/m² by using Eq. (1). Note that four interfaces between the Nd-Fe blocks and the Fe layers exist in the case of Fig. 4 (a). The parallel couplings compete with anti-parallel couplings between Nd-Fe blocks, $J_{\text{NdFe}/\text{NdFe}}$, which have opposite sign and comparable magnitude (e.g., $J_{\text{NdFe}/\text{NdFe}} \simeq J = 8.7$ mJ/m² for $\text{Nd}_6\text{Fe}_{13}\text{Ga}$ in Table I). As a result, one can under-

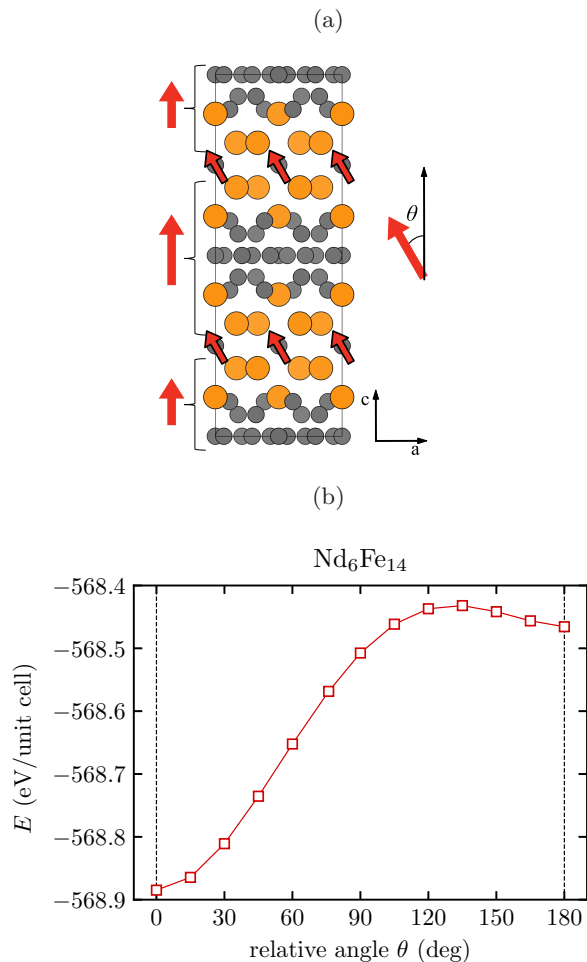


FIG. 4. (a): Assumed magnetic structure in $\text{Nd}_6\text{Fe}_{14}$, where the magnetic moments in the Fe layer have a relative angle θ to those in the Nd-Fe blocks. (b): Calculated energy per unit cell in $\text{Nd}_6\text{Fe}_{14}$ as a function of θ .

stand that the magnetic order of $\text{Nd}_6\text{Fe}_{14}$ is sensitive to the atomic positions (see Fig. 2 (c)).

From the above evaluation of the strength of magnetic couplings, we conclude that the cancellation of two kinds of magnetic coupling, $J_{\text{NdFe}/\text{NdFe}}$ and $J_{\text{NdFe}/\text{Fe}}$, induces the small energy difference observed between the FM and AF states in $\text{Nd}_6\text{Fe}_{14}$. On the other hand, $\text{Nd}_6\text{Fe}_{13}\text{Ga}$ has a single stable AF state because only the $J_{\text{NdFe}/\text{NdFe}}$ has a considerable effect in the $\text{Nd}_6\text{Fe}_{13}\text{Ga}$ structure.

In summary, we found that the substitution of Fe atoms in $\text{Nd}_6\text{Fe}_{14}$ by Ga atoms, leading to $\text{Nd}_6\text{Fe}_{13}\text{Ga}$, makes the AF state much stable, while $\text{Nd}_6\text{Fe}_{14}$ alloy favours ferromagnetic with a slight energy difference. We also reveal that this stable AF state originates from the anti-parallel coupling between the neighbouring Nd-Fe blocks and non-magnetic doped Ga atoms contributes to the stabilization of this magnetic state. It may be possible to consider that the enhancement of coercivity

of Nd-Fe-B magnets due to the addition of Ga atoms is related to the realization of AF state of $\text{Nd}_6\text{Fe}_{13}\text{Ga}$ alloy. The formation of AF state in the GB phase could block the domain wall propagation or suppress the nucleation of reversed domains within the GB phases.

ACKNOWLEDGMENTS

This work was supported by JST-CREST and the Elements Strategy Initiative Project (ESICMM) under the auspices of MEXT. Private communications with T. T. Sasaki, S. Doi, Y. Harashima, and S. Hirosawa are also appreciated.

- ¹S. Jonen, H. R. Rechenberg, *J. Appl. Phys.* **81**, 4054 (1997).
- ²S. Jonen, H. R. Rechenberg, *J. Appl. Phys.* **85**, 4448 (1999).
- ³H. S. Li, B. P. Hu, J. M. Cadogan, J. M. D. Coey, J. P. Gavigan, *J. Appl. Phys.* **67**, 4841 (1990).
- ⁴P. Schrey, M. Velicescu, *J. Magn. Magn. Mater.* **101**, 417 (1991).
- ⁵T. Kajitani, K. Nagayama, T. Umeda, *J. Magn. Magn. Mater.* **117**, 379 (1992).
- ⁶J. M. D. Coey, Q. Qi, K. G. Knoch, A. Leithe-Jasper, P. Rogl, *J. Magn. Magn. Mater.* **129**, 87 (1994).
- ⁷F. Pourarian, *Phys. B* **321**(1-4), 18 (2002).
- ⁸T. Sasaki, T. Ohkubo, Y. Takada, T. Sato, A. Kato, Y. Kaneko, and K. Hono, *Scr. Mater.* **113**, 218 (2016).
- ⁹K. G. Knoch, A. Le Calvez, Q. Qi, A. Leithe-Jasper, J. M. D. Coey, *J. Appl. Phys.* **73**, 5878 (1993).
- ¹⁰B. P. Hu, J. M. D. Coey, H. Klesnar, P. Rogl, *J. Magn. Magn. Mater.* **117**, 225 (1992).
- ¹¹Q. W. Yan, P. L. Zhang, X. D. Sun, B. P. Hu, Y. Z. Wang, X. L. Rao, G. C. Liu, C. Gou, D. F. Chen, Y. F. Cheng, *J. Phys.: Condens. Matter* **6**, 3101 (1994).
- ¹²P. Schobinger-Papamantellos, K. Buschow, and C. Ritter, *J. Alloys. Compd.* **359**, 10 (2003).
- ¹³J. Allemand, A. Letant, J. Moreau, J. Noziers, and R. D. L. Bathie, *J. Less-Common Met.* **166**, 73 (1990).
- ¹⁴C. H. de Groot, K. H. J. Buschow, and F. R. de Boer, *Phys. Rev. B* **57**, 11472 (1998).
- ¹⁵F. Weitzer, A. Leithe-Jasper, P. Rogl, K. Hiebl, A. Rainbacher, G. Wiesinger, J. Friedl, F. E. Wagner, *J. Appl. Phys.* **75**, 7745 (1994).
- ¹⁶O. Isnard, G. J. Long, D. Hautot, K. H. J. Buschow, and F. Grandjean, *J. Phys.: Condens. Matter* **14**, 12391 (2002).
- ¹⁷P. Schobinger-Papamantellos, K. H. J. Buschow, C. H. de Groot, F. R. de Boer, G. Böttger, and C. Ritter, *J. Phys.: Condens. Matter* **11**, 4469 (1999).
- ¹⁸J. Q. Li, W. H. Zhang, Y. J. Yu, F. S. Liu, W. Q. Ao, and J. L. Yan, *J. Alloys Compd.* **487**, 116-120 (2009).
- ¹⁹K. Momma and F. Izumi, *J. Appl. Crystallogr.* **44**, 1272 (2011).
- ²⁰G. Kresse and J. Furthüller, *Phys. Rev. B* **54**, 11169 (1996).
- ²¹P. E. Blöchl, *Phys. Rev. B* **50**, 17953 (1994).
- ²²G. Kresse and D. Joubert, *Phys. Rev. B* **59**, 1758 (1999).
- ²³J. P. Perdew, J. A. Chevary, S. H. Vosko, K. A. Jackson, M. R. Pederson, D. J. Singh, and C. Fiolhais, *Phys. Rev. B* **46**, 6671 (1992).
- ²⁴R. F. W. Bader, *Atoms in Molecules: A Quantum Theory*. (Oxford University Press, Oxford, 1990).
- ²⁵W. Tang, E. Sanville, G. Henkelman, *J. Phys.: Compute Mater.* **21**, 084204 (2009).
- ²⁶S. Doi (private communication).
- ²⁷Y. Harashima, K. Terakura, H. Kino, S. Ishibashi, and T. Miyake, *J. Appl. Phys.* **120**, 203904 (2016).
- ²⁸O. K. Andersen, *Phys. Rev. B* **12**, 3060 (1975)